Bioorganic & Medicinal Chemistry 20 (2012) 5053–5061

Contents lists available at SciVerse ScienceDirect

Bioorganic & Medicinal Chemistry

journal homepage: www.elsevier.com/locate/bmc

Bioengineering functional copolymers. XXI. Synthesis of a novel end carboxyl-trithiocarbonate functionalized poly(maleic anhydride) and its interaction with cancer cells

Zakir M. O. Rzayev [a,*], Mustafa Tűrk [b], Ernur A. Söylemez [a,c]

[a] Institute of Science & Engineering, Division of Nanotechnology and Nanomedicine, Hacettepe University, Beytepe 06800, Ankara, Turkey
[b] Department of Biology, Faculty of Arts and Sciences, Kirikkale University, Yahşihan 71450, Kirikkale, Turkey
[c] Department of Chemistry, University at Buffalo, The State University of New York, Buffalo, NY 14260-3000, USA

ARTICLE INFO

Article history:
Received 7 February 2012
Revised 21 May 2012
Accepted 25 May 2012
Available online 5 June 2012

Keywords:
Synthesis
RAFT polymerization
Multifunctional polymer
Cancer cells
Cytoxicity
Apoptotic and necrotic effects

ABSTRACT

A novel carboxyl-trithiocarbonate functionalized polymer with a highly selective antitumor activity was synthesized by a reversible addition-fragmentation chain transfer (RAFT) polymerization of maleic anhydride (MA) with benzoyl peroxide as an initiator and S-1-dodecyl-S-(α,α′-dimethyl-α″-acetic acid)-trithiocarbonate as a RAFT agent with the aim to design and synthesize an effective anticancer agent with minimum side effects. The structure, molecular weights and composition of synthesized polymers were investigated by ^{1}H (^{13}C) NMR, MALDI-TOF-MS and GPC analyzes. It was demonstrated that RAFT polymerization of MA was accompanied by a partially controlled decarboxylation of anhydride units and the formation of conjugated double bond fragments in backbone macromolecular chains. The mechanism of interaction of pristine RAFT agent and PMA–RAFT polymer with cancer (HeLa human cervix carcinoma) and normal (L929 Fibroblast) cells was investigated by using a combination of chemical, biochemical, statistical, spectroscopic (SEM and fluorescence inverted microscope) and real-time analysis (RTCA) methods. PMA–RAFT exhibited higher and selective cytotoxicity, apoptotic and necrotic effects toward HeLa cells at relatively low concentrations (around 7.5–75 μg mL^{-1}, IC_{50} = 11.183 μg mL^{-1}) and toward Fibroblast cells at high concentrations (IC_{50} >100 μg mL^{-1}). The observed highly selective antitumor activity render PMA–RAFT polymers as promising candidates for the utilization in cancer chemotherapy.

1. Introduction

Many natural polymers such as poly(lysine), poly(arginine), dextran derivatives, heparin and chitosan, and synthetic carboxyl functionalized polymers such as poly(acrylic acid), copolymers of maleic anhydride, have now been reported to have direct or indirect antitumor activity via stimulation of the immune system.[1–4] In recent years, the acrylic acid homo- and copolymers have been often used as carriers in drug release systems, because of their multifunctional nature, unique properties and good biocompatibility.[5,6] The polymers, containing carboxylic groups, exhibit a swelling behavior depending on pH and ionic strength of solution.[7,8] Argentiere et al.[9] investigated poly(acrylic acid) (PAA) nanogels as pH-sensitive carriers for biomedical applications. They prepared PAA–biopolymer nanogels by loading and release of an oligothiophene fluorophore and its albumin conjugate onto the PAA macromolecules.

Synthesis of thiazole-containing low molecular weight compounds as potential antitumor agents was a subject of numerous investigations.[10–14] In some early publications, the synthesis of a series of 2,4-disubstituted thiazole derivatives bearing *N*-*n*-butyl or *N*-cyclohexylthioureido synthon[10] and a number of imidazole[2,1-*b*]thiazoles[11] and their spectroscopic, biological and testing results for antitumor activity were reported. The thiazole derivatives showed antineoplastic activity at concentrations less than 100 μM with GI_{50} (mean-graph midpoint) of around 17.8–7.4 μM. According to the authors, ethyl 2-[3-(diethylaminopropanamido]-thiazole-4-carboxylate showed remarkable activity against leukemia cell line with a GI_{50} value of 0.08 μM, and a broad spectrum activity toward all tumor cells at 38.3 μM concentration.[12] The imidazole[2,1-*b*]thiazoles were tested in mice bearing Enrlich as cites tumor cells. Authors found that the nitrogen mustard for some compounds had a T/C of 140 at 8 mg/kg. Other researchers also reported the clinical testing of the thiazole nucleoside thiazofum.[15,16] Husain and Ajmal[17] synthesized a novel series of 2-[3-(4-bromophenyl) propan-3-one]-5-(substituted phenyl)-1,3,4-oxadiazoles from 3-(4-bromobenzoyl) propionic acid and evaluated their anti-inflammatory, analgesic, ulcerogenic and antibacterial activities. They found that 1,3,4-oxadiazole nucleus resulted in increased anti-inflammatory and analgesic activities with a significant decrease of ulcerogenic activity. Akhtar et al.[18] synthesized novel benzothiazole derivatives and investigated their in vitro antitumor activity.

* Corresponding author. Tel.: +90 312 297 6439; fax: +90 312 299 2124.
E-mail address: zmo@hacettepe.edu.tr (Z.M.O. Rzayev).

0968-0896/$ - see front matter © 2012 Elsevier Ltd. All rights reserved.
http://dx.doi.org/10.1016/j.bmc.2012.05.058

Authors tested obtained compounds against representatives of several virus families containing single stranded RNA genomes, either positive-sense (ssRNA$^+$) or negative-sense (RNA$^-$), and against double-stranded RNA genomes (dsRNA), as well as some Flaviviridae viruses. According to the authors, some benzothiazole derivatives showed strong effect on leukemia cell lines CCRF-CEM (CC_{50} 12 ± 2 and 8 ± 1 mmol L^{-1}, respectively). Some heterocyclic S- and N-containing compounds such as thiophenecarbohydrazide, thieno-pyrazole and thienopyrimidine derivatives were synthesized by Abu-Hashem et al.[19] Based on pharmacological testing results, the authors showed that these compounds exhibit significant antitumor and antioxidant activity.

In addition to several well-known drug delivery strategies developed to facilitate effective chemotherapy with anticancer agents, some new approaches have been recently established. Various approaches such as drug modifications and development of new carrier systems for anti-cancer agents have been attempted to enhance their tumor reach. According to Reddy,[20] approaches such as drug delivery through enhanced permeability and retention (EPR) effect have resulted in a significant improvement in concentration in tumors, while approaches such as drug-carrier implants and microparticles have resulted in improvement in local chemotherapy of cancer. The author discussed different strategies employed for the delivery of anti-cancer agents to tumors, such as through the EPR effect, local chemotherapeutic approaches using drug delivery systems, and special strategies such as receptor-mediated delivery, pH-based carriers, application of ultrasound and delivery to resistant tumor cells and brain using nanoparticles. Bešić[21] reported newly developed methods of drug delivery to tumors and of the related anticancer therapies based on the combined use of different physical methods and specific drug carriers. According to the author, conventional strategies and new approaches have been put into perspective to revisit the existing and to propose new directions to overcome the threatening problem of cancer diseases.

Recently, Lonkar and Dedon[22] reported a new approach and concept to solve the problems of the mechanistic link between chronic inflammation (as a risk factor for many human cancers), DNA damage and cancer. The authors described important roles of free radicals and reactive species such as nitric oxide, oxygen, and peroxide species in cell signaling and apoptosis, as well as physiological and pathological pathways mediated by chemical mediators of inflammation. The mechanisms of these processes were arbitrarily divided into biological and chemical. According to the authors, the full spectrum of chemistries possible with the reactive species generated by phagocytes likely plays a substantial role in the carcinogenic process. Tong and Cheng[23] described the current state of the preclinical and clinical investigations of pH-sensitive polymer–drug conjugates and polymer nanoparticles for targeted cancer therapy. According to the authors, modern polymer chemistry makes it possible for the synthesis of a large variety of synthetic polymer materials for the cancer drug delivery. Many researchers focused on the investigation of DNA interactions with cationic polymers, polyelectrolytes and surfactants, results of which summarized in recent published book.[24]

The progress in the knowledge of the mechanism of radical polymerization has led to the synthesis of a large variety of well-defined polymers, especially polymers with functionalized end-groups.[25] Recent developments in the field of controlled/living radical polymerization (CRP) has led to the re-evaluation of many generally held concepts of living polymerization. CRP employs the principle of creation and exploitation of an equilibration between active growing free radicals and various types of dormant species.[25,26] Reversible addition-fragmentation chain transfer (RAFT) along with other known CRP methods offer significant versatility in providing polymers with well-controlled molecular weights and narrow molecular weight distributions,[27,28] which facilitates the design of various polymeric nanostructures.[29–35]

The synthesis of carboxyl/anhydride, pyran and boron containing copolymers, their various modifications and the investigation of their interactions with cancer cells were subjects of our recent publications.[36–39] In the present work, we report the synthesis of novel carboxyl-trithiocarbonate end-chain functionalized polymers with unique structure and properties, such as a narrow molecular weight distribution, solubility and reactivity in aqueous medium. The synthesized end-functionalized polymers exhibit a combination of important properties such as amphiphilicity, biocompatibility, reactivity toward free radicals and other reactive species, capability to achieve conjugation with biomolecules via carboxyl-amine H-bonding, and the reactivity toward DNA through trithiocarbonate-amine chemical reactions.

The goal of this work is to synthesize and characterize a new class of carboxyl-trithiocarbonate functionalized polymers by RAFT polymerization of MA with BP as a radical initiator and S-1-dodecyl-S-(α,α′-dimethyl-α″-acetic acid)trithiocarbonate as the RAFT agent. An important aspect of this work is comparative investigations of the interactions of synthesized water-soluble and biocompatible reactive surfactants such as pristine RAFT compound and PMA–RAFT polymer with HeLa (human cervix carcinoma cell) cancer cells and L929 Fibroblast normal cells, and evaluation of their antitumor activity (cytotoxicity, apoptotic and necrotic effects) by using a combination of different methods such as real-time analysis, statistical, hematoxylen/eosin and immunocytochemical staining, light and fluorescence inverted microscopy analyzes.

2. Experimental

2.1. Materials

MA monomer (Fluka) was purified before use by re-crystallization from anhydrous benzene solution and sublimation in vacuum. S-1-dodecyl-S-(α,α′-dimethyl-α″-acetic acid)trithiocarbonate as a RAFT agent-surfactant was synthesized by a literature procedure[40] and purified by re-crystallization from hexane solution. Benzoyl peroxide as a radical initiator (Aldrich–Sigma, Germany) was purified before use by re-crystallization twice from benzene solution. HeLa (human cervix carcinoma cell) cancer cells and L929 Fibroblast cells were obtained from the tissue culture collection of the SAP Institute (Turkey). Cell culture flasks and other medical plastic materials were purchased from Corning (Israel). The growth medium, which is Dulbecco modified medium (DMEM) without L-glutamine supplemented fetal calf serum (FCS), and trypsin-EDTA were purchased from Biological Industries (Israel). The primary antibody, caspase-3 was purchased from Lab Vision.

2.2. Synthetic procedure

S-1-Dodecyl-S-(α,α′-dimethyl-α″-acetic acid)trithiocarbonate (RAFT agent) was synthesized by a known synthetic procedure.[40] After recrystallization from hexane solution, yellow crystalline product was obtained with a mp of 62.5 °C (by DSC analysis). Structure of this RAFT agent was confirmed by ^{1}H (^{13}C) NMR spectroscopy: ^{1}H NMR spectra (in $CHCl_3$-d_1), δ (ppm): CH_2–C**H$_3$** 0.88 and $(CH_2)_n$ 1.35–1.26 in end alkyl group, α –CH_2-S 3.27, β –CH_2–CH_2-S 1.66 and γ –C**H$_2$**–CH_2–CH_2-S 1.38 in end octadecyl group, 2C**H$_3$** 1.71. ^{13}C NMR spectra (in $CHCl_3$-d_1), δ (ppm): **C**H$_3$ 14.11 and (**C**H$_2$)$_n$ 29.64–28.98 in end alkyl group, α –**C**H$_2$-S 55.66, β –**C**H$_2$–CH_2-S 27.83 and γ –**C**H$_2$–CH_2–CH_2-S 31.92 in end octadecyl group, **C**=S 77.79 in end trithiocarbonate linkage, –**C**=O in –COOH 179.14, 2**C**H$_3$ and *t*-**C** in end group 25.22 and 37.07, respectively.

Decarboxylated PMA–RAFT polymer was synthesized by RAFT heterogeneous polymerization of MA monomer in toluene under

a nitrogen atmosphere in the presence of BP as a radical initiator and the RAFT agent. Reaction conditions: [MA] = 2.55 mol L^{-1}, [BP] = 2.58×10^{-2} mol L^{-1}, [RAFT] = 8.34×10^{-3} mol L^{-1} and toluene 10 mL; temperature 80 °C, reaction time 16 h. The reaction mixture was cooled in liquid nitrogen and degassed in a round-bottom flask equipped with condenser and magnetic stirrer, then refluxed under nitrogen atmosphere during reaction. Precipitation of the formed polymer during reaction was observed. The product was isolated centrifugation, purified by precipitation from acetone solution with toluene and washed with hexane. The purple-brown colored paraffin-like product was dried under vacuum at 40 °C for 6 h.

^{1}H NMR spectrum (in $CHCl_3$-d_1), δ (ppm): C**H$_3$** 0.88 and $(CH_2)_n$ 1.68–1.47 (broad peak) in end alkyl group, α –C**H$_2$**-S 3.49, β –C**H$_2$**–CH_2-S 2.05 and γ –C**H$_2$**–CH_2–CH_2-S 1.94 in end octadecyl group, 2C**H$_3$** in end isopropyl group 1.31, backbone –C**H**–C**H**– 4.01 and 3.92, backbone conjugated –C**H**≡C**H**– 7.03, proton from end –COO**H** group 7.52.

^{13}C NMR spectrum (in $CHCl_3$-d_1), δ (ppm): –**C**≡O in –**C**OOH 167.5, 2**C**H_3 and *t*-**C** in end group 29.62 and 34.31, respectively, backbone –**C**H–**C**H– 77.76, –**C**≡O in anhydride units 164.14, backbone conjugated –**C**H≡**C**H– 136.82, **C**≡S 65.2 in end trithiocarbonate linkage, α –**C**H_2-S 42.66, β –**C**H_2–CH_2-S 37.21 and γ –**C**H_2–CH_2–CH_2-S 31.9, (**C**H_2)$_n$ 29.42 and **C**H_3 14.11 in end octadecyl group.

2.3. Characterization

^{1}H and ^{13}C NMR spectra of RAFT agent and PMA–RAFT polymer were performed on a Bruker Avance (400 MHz) NMR spectrometer (Germany) with $CHCl_3$-d_1 as a solvent at 25 °C. Average-number, average-weight and average-viscosity molecular weights (M_n, M_w and M_v) and molecular weight distribution (M_w/M_n) of PMA–RAFT polymer were determined by GPC chromatography. GPC analysis was carried out on Viscotek's GPCMax with two PolyPore columns (Varian Inc.) and TDA302 tetradetector array system which contained refractive index, UV, viscosity, and low (7°) and right angle light scattering modules. THF was used as a carrier solvent at 30 °C. The system was calibrated before measurements with polystyrene standards. MS analysis was performed on a Voyager DE PRO MALDI-TOF-MS spectrometer using dithranol as a matrix and NaTFA salt as a cationizing agent for ionization of the sample.

2.4. Cytotoxicity

Cytotoxicity was determined using the real-time analyzer (RTCA) SP instrument (Roche, Germany) to monitor cellular responses after treatment with the anti-cancer agents in vitro. HeLa and L929 Fibroblast cells (10×10^3 cells per well) were cultivated in DMEM-F12 without L-glutamine using E-Plate 96 (Roche) for cell growth monitoring. The plates were kept in the CO_2 incubator (37 °C in 5% CO_2) during the experiment. After 19 h of incubation, different amounts of RAFT, PMA–RAFT (about 0.78–100 μg mL^{-1} in the medium) were added into the wells containing cells and cultivated at the same conditions. The attachment and logarithmic growth of the cells was monitored every 30 min over 45 h.

2.5. Analysis of apoptotic and necrotic cells

Double staining was performed to quantify the number of apoptotic cells in the culture based on scoring apoptotic cell nuclei. HeLa cells (20×10^3 cells per well) were grown in DMEM-F12 without L-glutamine supplemented with 10% fetal bovine serum and 1% penicillin–streptomycin at 37 °C in a 5% CO_2 humidified atmosphere by using 24-well plates. HeLa cells were treated with different amounts (0, 7, 5, 15, 30, 50 and 75 μg mL^{-1}) of RAFT agent and the same amount of PMA–RAFT for 24 h. Additionally, cancer cells were treated with only cell medium as a control. Both attached and detached cells were collected, then washed with PBS and stained with Hoechst dye 33342 (2 μg mL^{-1}), propodium iodide (PI) (1 μg mL^{-1}) and free-RNAse DNAse (100 μg mL^{-1}) for 15 min at room temperature. Then, 10–50 μL of cell suspension was smeared on the slide and cover slip for examination using fluorescence microscopy. The number of apoptotic and necrotic cells were determined by fluorescence inverted microscope DMI6000 (Leica) with DAPI filter, and FITC filter.[36]

2.6. Immunocytochemical stains

Approximately 2 mL of HeLa cells (20×10^3 cells per well) were treated with the RAFT agent and PMA–RAFT (around 0–75 μg mL^{-1}). Cancer cells were also treated with only cell medium as a control. For an indirect immunocytochemistry procedure, cytology specimens were treated with 3% H_2O_2 for 10 min, diluted with water, and then rinsed in PBS (pH 7.4) for 5 min. The primary antibody, caspase-3 (Lab Vision), was diluted at 1:300, and then incubated for 1 h at room temperature. Specimens were washed with a PBS buffer (pH 7.4) and incubated in the biotinylated secondary antibody solution for 10 min. For the negative control, the primary antibody was omitted in one of the slides. The immune reactivity of the caspase-3 antibody is confined to the cytoplasm of apoptotic cells. The number of the caspase-3-positive cytoplasm stained cells in all fields were found at ×400 final magnification. For each image (at least 100 cells/field), three randomly selected microscopic images were evaluated.[36]

2.7. Statistical analysis

Cytotoxicity, apoptosis and necrosis studies were performed in triplicate. The results were represented as mean ± standard deviation (SD), and analyzed using the independent samples *t*-test (for two groups). Statistical significance was set at $P < 0.05$.

3. Results and discussion

3.1. Design and structure of end-functionalized polymer

The synthetic pathway for the preparation of the end-chain carboxyl-trithiocarbonate functionalized polymer can be represented as follows (Fig. 1):

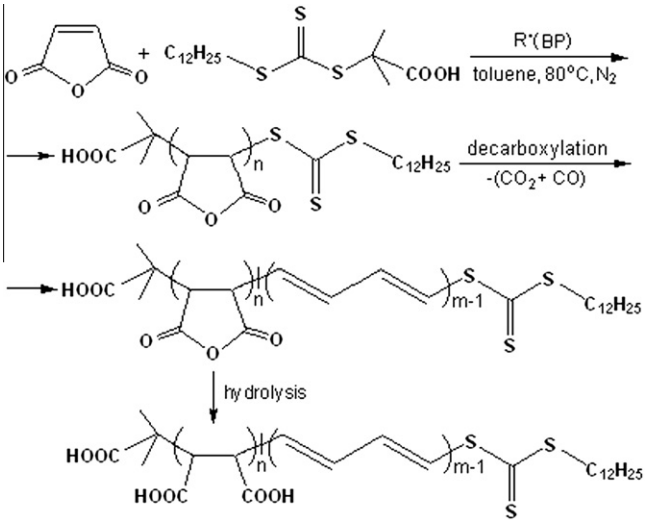

Figure 1. RAFT polymerization of maleic anhydride.

The structure of the synthesized carboxyl-trithiocarbonate containing RAFT agent and PMA–RAFT polymer was investigated by ^{1}H (^{13}C) NMR spectroscopy analyzes, which are provided in Figures 2 and 3.

The monomer unit molar ratio (m_1/m_2) and the amount of end functional groups in partially decarboxylated polymer was calculated using NMR analysis (Table 1) and the following equation:

$$m_1/m_2 = n_2 Am_1(CH{=}CH)/n_1 Am_2(C{=}O \quad \text{or} \quad CH) \qquad (1)$$

where Am_1 and Am_2 are the normalized areas per H (or C) from the corresponding functional groups of the monomer unit regions in ^{1}H (^{13}C) NMR spectra; n_1 and n_2 are the integers of proton(s) or carbon(s) in the functional group of the monomer units; total molar fraction of repeat units, including two end groups (E_1 and E_2) with different functionalities $E_1-(m_1 + m_2)-E_2 = 1$.

The obtained results suggest that RAFT polymerization of MA is accompanied by a side-chain decarboxylation and a formation of conjugated double bonds in the main backbone chain as shown in Figure 4 with MALDI-TOF-MS spectra. The obtained mass parameters of the polymer sample suggest the formation of an oligomeric structure with the mass of repeated unit 173 m/z and an average mass of 4408 m/z including of the mass of end functionalized segments. As seen from these results, the radical RAFT polymerization of MA is accompanied by transformation of anhydride units to the conjugated double bond fragments in the main backbone concurrent with the chain growing and termination reactions.

From to the results of NMR analysis (Table 1), the content of conjugated double bonds as a second monomer unit (m_2) is equal to 82 mol %, which indicates a significant controlled decarboxylation of anhydride units (m_1) during RAFT polymerization and the formation of conjugated double bonds on main chain as a second repeat unit (m_2). The isolated and purified polymer is purple–brown paraffin-like product presumably due to its backbone conjugated structure and low molecular weight. Similar but non-controlled decarboxylation was also observed by many researchers in conventional radical,[41–43] ionic[44,45] and catalytic (Al_2O_3–TiO_2)[46] polymerizations of MA. Ryan et al.[47] reported the formation of only anhydride units in the polymer chain when authors utilized a pulsed plasma technique for the polymerization of MA.

The average-number, average-weight and average-viscosity molecular weights (M_n, M_w and M_v) and molecular weight distribution (M_w/M_n) of PMA–RAFT polymer were determined by GPC chromatography (Fig. 5), the values of which were summarized in Table 1. As seen from these results, PMA–RAFT polymer exhibited low polydispersity (PI = 1.126), which is an important parameter for the functional copolymers utilized in biological applications.

3.2. Evaluation of cytotoxicity

The cytotoxicities of the RAFT agent and the PMA–RAFT copolymers were evaluated on HeLa and L929 Fibroblast cell lines. According to RTCA system results, the copolymer concentration had a strong impact on cell mortality. The cytotoxicity was determined as a half-maximum inhibiting concentration (IC_{50}) values from the resulting dose-response curves (Fig. 6). As seen from these results, the RAFT agent was more toxic to HeLa and Fibroblast cells than the PMA–RAFT copolymer. IC_{50} values of the RAFT agent were 0.794 μg mL^{-1} for HeLa cells and 0.464 μg mL^{-1} for Fibroblast cells in vitro. IC_{50} values of the PMA–RAFT copolymer were 11.183 μg mL^{-1} for HeLa cells and higher than 100 μg mL^{-1} for Fibroblast cells in vitro. The toxicity effect (decrease of the cell index) was observed 2 h after the addition of the RAFT agent and the PMA–RAFT copolymer (Fig. 7A and B). On the other hand, the cell index of control samples and PMA–RAFT treated Fibroblast (Fig. 7B) groups (showed in Fig. 7 by arrows) increased after another 24 h. Thus, the RAFT agent was found to be more cytotoxic to HeLa and Fibroblast cells than the PMA–RAFT copolymer. Importantly, the PMA–RAFT copolymer exhibited cytotoxicity toward HeLa cells, but not toward Fibroblast (normal cells) in vitro. These

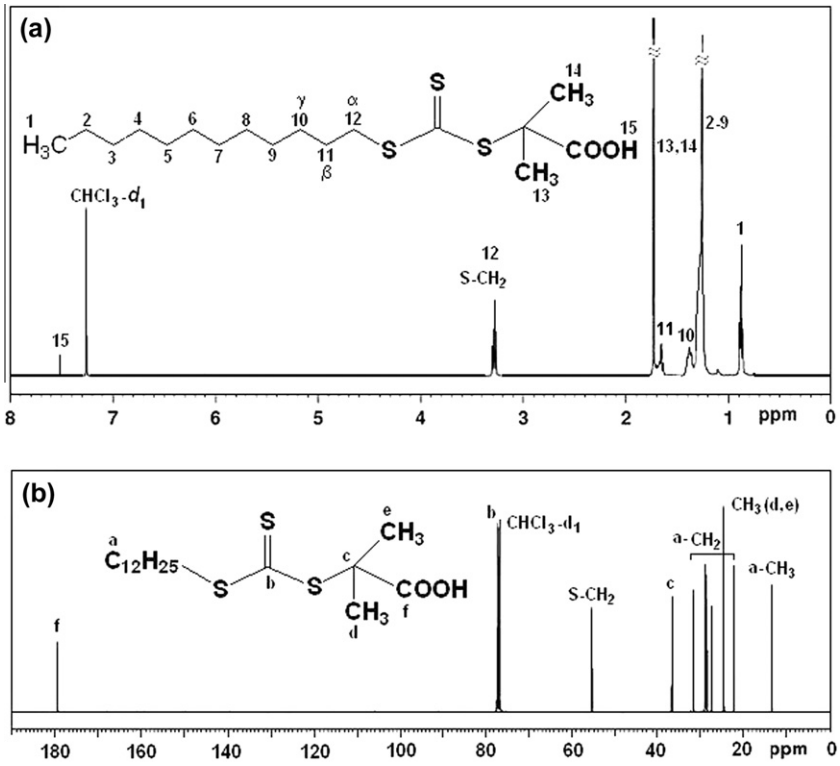

Figure 2. (a) ^{1}H NMR and (b) ^{13}C NMR spectra of S-1-dodecyl-S-(α,α′-dimethyl-α″-acetic acid)trithiocarbonate (RAFT agent) in $CHCl_3$-d_1.

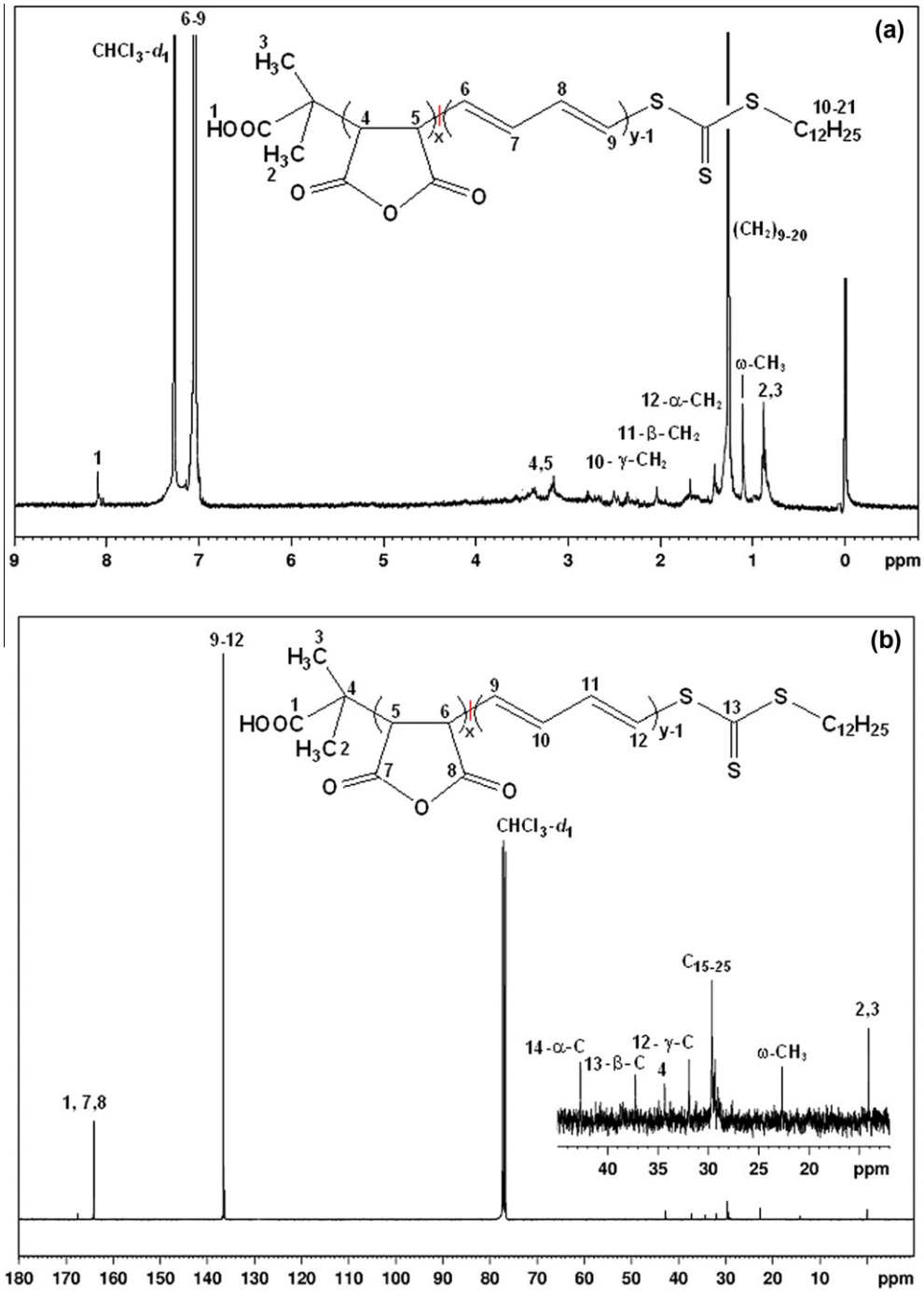

Figure 3. (a) ^{1}H NMR and (b) ^{13}C NMR spectra of decarboxylated PMA–RAFT copolymer in $CHCl_3$-d_1.

Table 1
Some structural parameters, composition, average molecular weights (M_n, M_w and M_z) and polydispersity (PI) of partially decarboxylated PMA–RAFT

NMR analysis	^{1}H	^{13}C	Monomer and end units in polymer[a] (mol %)		Average molecular weights (g/mol)
$A_{C=O}$ or A_{CH-CH} δ (ppm)	4.0–3.92	164.14	m_1 (MA unit)	14.35	M_n 3028
$A_{CH=CH}$ δ (ppm)	7.03	136.52	m_2 (CH=CH unit)	82.39	M_w 3410
Peak area/intensity (cm) Am_1 (C=O or CH–CH)	4.23	2.05	End-*i*-propyl group	0.77	M_z 3.826
Peak area/intensity (cm) m_2 (CH=CH)	4.04	11.77	End-*n*-octadecyl group	2.49	PI (M_w/M_n) = 1.126

[a] Total intensity of carbon atoms in polymer is 14.285 cm.

observations suggest that the designed and synthesized PMA–RAFT copolymer containing carboxyl/trithiocarbonate linkages exhibits higher cytotoxicity at relatively lower concentration with minimum side effects.

3.3. Apoptosis results

The apoptotic ratio was obtained in two different ways: firstly by caspase-3 immunostaining and secondly by double staining

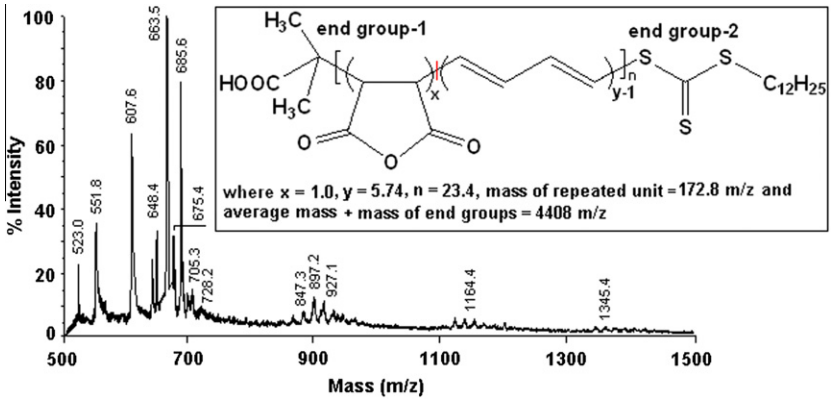

Figure 4. MALDI-TOF-MS spectra of end functionalized and decarboxylated PMA.

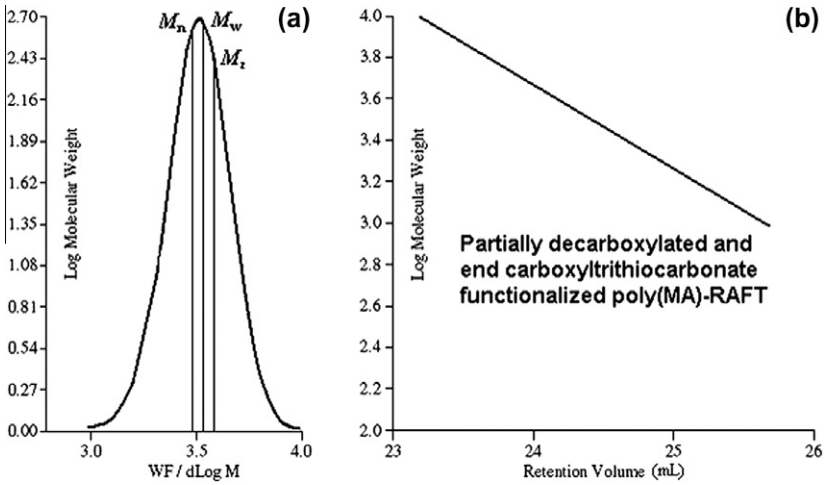

Figure 5. GPC analysis, average molecular weights (M_n, M_w and M_z) and the polydispersity index (PI) for multifunctional poly(MA)-RAFT copolymer.

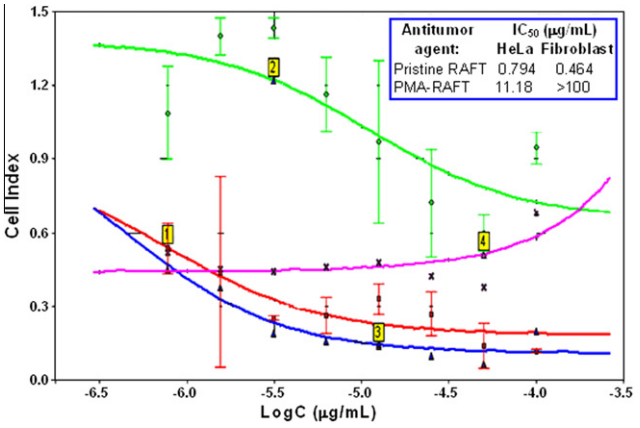

Figure 6. Cytotoxicity (IC_{50}) of the RAFT agent and the PMA–RAFT copolymer toward HeLa and L929 Fibroblast cells from plots of cell index versus log*C* (the logarithm of the RAFT agent and PMA–RAFT concentrations): (1) HeLa cells treated with the RAFT agent; (2) HeLa cells treated with PMA–RAFT copolymer; (3) Fibroblast cells treated with the RAFT agent and (4) Fibroblast cell treated with the PMA–RAFT copolymer. Average IC_{50} values are presented in the inset table of this figure. All plots were generated using the RTCA Software 1.1. IC_{50} values were calculated after 45 h.

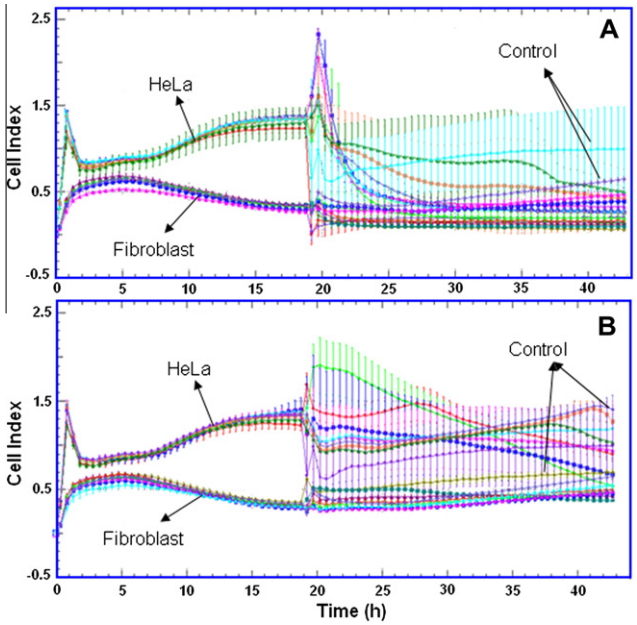

Figure 7. Dynamic monitoring of HeLa and Fibroblast cells treated with the RAFT agent and the PMA–RAFT copolymer using the real-time analyzer (RTCA). Cell index monitored every 30 min for 45 h; 19 h later, cells were treated with the RAFT agent and the PMA–RAFT copolymer (0.78–100 μg mL^{-1}) in E-plates 96: (A) HeLa and Fibroblast cells treated with RAFT and (B) HeLa and Fibroblast cells treated with the PMA–RAFT copolymer. Controls include only cell culture medium.

method. The average values obtained by using these methods are summarized in Table 2, while light and fluorescence microscope images are provided in Figure 8. An apoptotic effect was observed

Table 2
Apoptotic and necrotic indexes obtained as a result of the interactions of (**I**) RAFT and (**II**) PMA–RAFT with different ratios in HeLa cell cultures. Statistical differences (P <0.05) for the apoptotic and necrotic activity between (**I**) and (**II**) samples were represented the mean ± SD

Amount of RAFT and PMA–RAFT in a well (μg mL^{-1})	Apoptotic index (%)		Necrotic index (%)	
	I	**II**	**I**	**II**
0.0	2 ± 1	1 ± 1	3 ± 1	2 ± 1
7.5	12 ± 2	34 ± 3	21 ± 2	7 ± 2
15	20 ± 2	46 ± 3	43 ± 3	13 ± 3
30	30 ± 3	62 ± 3	65 ± 4	18 ± 3
50	25 ± 3	71 ± 4	74 ± 3	24 ± 4
75	13 ± 2	56 ± 5	86 ± 4	45 ± 5

at low concentrations for both the RAFT agent and the PMA–RAFT copolymer, but increased at higher polymer concentrations. For the RAFT agent, the apoptotic effect increased for concentrations up to 30 μg mL^{-1} (Table 2) but decreased by 10–15% at high concentrations (50 μg mL^{-1} and above). The latter result was attributed to the increased cytoxicity at higher RAFT agent concentrations. Additionally, a stronger apoptotic effect was observed at elevated PMA–RAFT concentrations compared to samples with a high concentration of the RAFT compound. Apoptosis can be clearly distinguished in the images obtained by caspase-3 immunostaining. In particular, Figure 8A reveals no brown color caused by caspase-3 staining in the cytoplasm, since there was no apoptosis in the control group; while Figure 8B shows a brown color in the cell cytoplasm due to the reaction by caspase-3 antibodies. Double

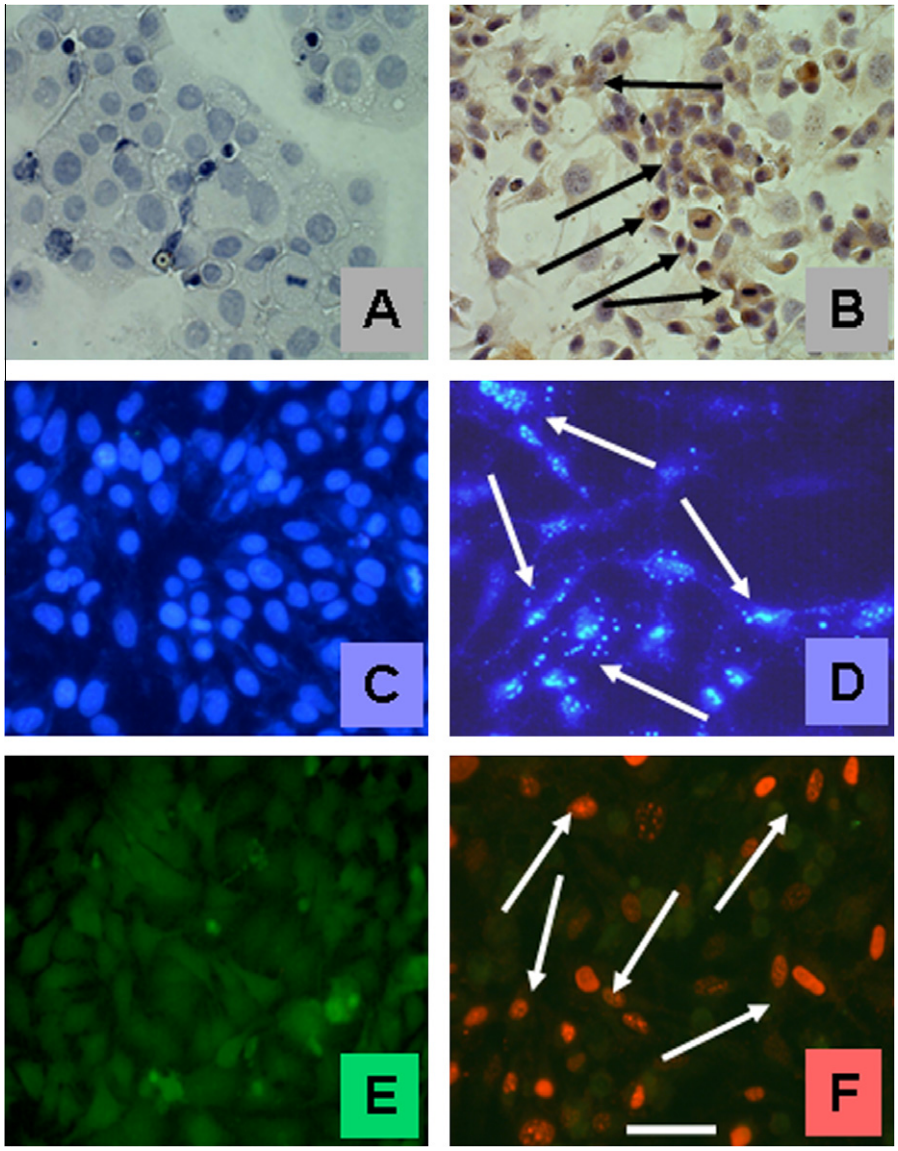

Figure 8. Apoptotic cell images of immunocytochemical staining performed by using caspase-3 antibody and double staining method with Hoechst 33342 as a fluorescent dye. Necrotic cell images were obtained by a double staining method performed by using propodium iodide (PI) fluorescent stain. (A) HeLa cells stained with caspase-3 (control group); (B) HeLa cells stained with caspase-3 exposed to the PMA–RAFT copolymer at a concentration of 50 μg mL^{-1}, where cells undergoin apoptosis are shown by arrows; (C) HeLa cells stained by Hoechst 33342 not treated with the polymer (control group); (D) HeLa cells stained by Hoechst 33342 and exposed to the PMA–RAFT copolymer at a concentration of 50 μg mL^{-1}, where cell nuclei undergoing apoptosis are shown by arrows; (E) HeLa cells stained by a double staining method and not treated with the polymer (control group); (F) HeLa cells exposed to the PMA–RAFT copolymer at a concentration of 50 μg mL^{-1}, where necrosed cell nuclei look red (shown by arrows) stained with PI and non-necrosed cell nuclei look green. Photographs were taken by Leica DMI6000 inverted fluorescent microscope at ×400 magnification. The scale shows a distance of 20 μm.

staining is another method used in determining apoptosis. Hoechst 33342 fluorescent stain used in this method penetrates through the membranes of living cells and stains the nucleus. As a result, nuclei are rendered blue when observed by the DAPI filter under a fluorescent microscope. This technique also enables the evaluation of nuclear morphology. The apoptotic index obtained by the double staining method is summarized in Table 2, and some of the images taken with an inverted fluorescence microscope are collected in Figure 8. The apoptotic effect, obtained in parallel with the results of caspase-3 immunocytochemical staining, can be clearly observed especially for wells where the PMA–RAFT copolymer was applied. Thus, for the samples with the PMA–RAFT copolymer, the apoptotic cell nuclei decomposed and appeared in brighter blue color compared to non-apoptosis cells (Fig. 8D). On the other hand, an image from the control group shows no morphological difference in cell nuclei (Fig. 8C). The apoptotic effect of the RAFT agent was lower compared to that of the PMA–RAFT copolymer. The highest apoptotic index of approximately 71 ± 4% was obtained for PMA–RAFT at 50 μg mL^{-1} concentration. There was a statistical difference (P <0.05) between the apoptotic effect observed for the RAFT agent and for the PMA–RAFT copolymer at each concentration.

3.4. Necrosis results

Propodium iodide (PI) is an intercalating fluorescent molecule that was used in the double staining method to detect necrosis in cancer cells subjected to interaction with the RAFT agent and the PMA–RAFT copolymer. This stain penetrates through dead cells and cells with damaged plasma membrane, and causes the nuclei to look red under fluorescent light. The nuclei of healthy and apoptotic cells look blue or green when scanned by an FITC fluorescent filter. In our study, the necrotic deviation index was examined under fluorescent light (by a FITC filter) at a wavelength of 480–520 nm, where necrotic cell nuclei appeared red and healthy or apoptotic cell nuclei appeared green. The images of necrotic cells are summarized in Figure 8F, and the necrotic percentage index is provided in Table 2. As seen from these results, the necrotic index is not very high at low concentrations of the RAFT agent or copolymer. However, at higher concentrations a significant increase in toxicity and necrosis was observed. It was determined that the RAFT agent had a particularly high necrotic effect. As shown in Table 2, the necrotic effect of the PMA–RAFT copolymer was weaker compared to the RAFT agent. The necrotic effect of the copolymer was found to be 45 ± 5% at 75 μg mL^{-1} concentration, while the necrotic index of approximately 86 ± 5% was obtained for the RAFT agent at 75 μg mL^{-1} concentration. There was a statistical difference (P <0.05) between the necrotic effects of the RAFT agent and the PMA–RAFT copolymer at each concentration.

The interaction pathways of the pristine RAFT agent and the PMA–RAFT copolymer with biomacromolecules can be represented as follows (Figs. 9 and 10).

We propose that the observed highly selective antitumor activity of the PMA–RAFT copolymer is related to the presence and distribution of carboxyl and trithiocarbonate groups, which are capable of physical (carboxyl-amine H-bonding) and chemical (trithiocarbonate-amine reaction and termination of free radicals and other reactive species) interactions within a biological environment, as well as its amphiphilic character. These important factors contribute to the inhibition of the cancer cell growth via destruction of supramacromolecular assemblies (Figs. 8–10). Additionally, the conjugated double bond segments of the PMA–RAFT copolymer may also participate in the reaction with free radicals, acting as an effective antioxidant. The evaluation of free radicals using electron spin resonance (EPR) analysis method and

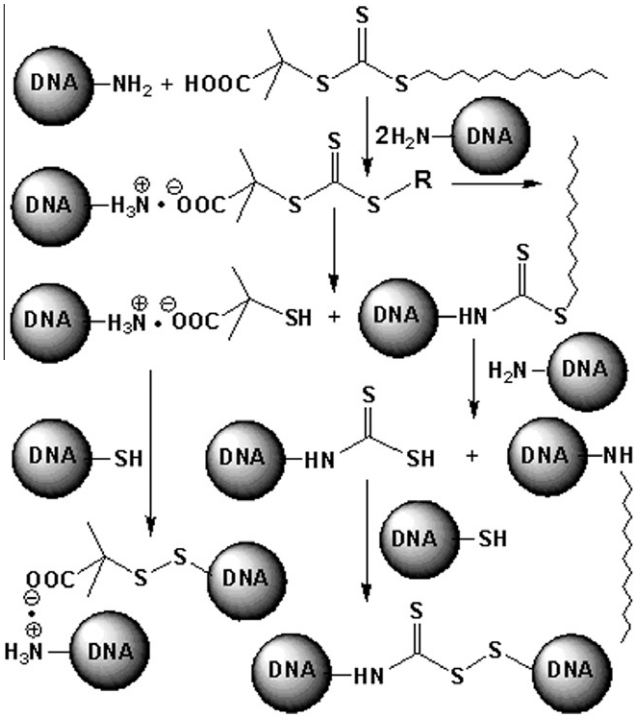

Figure 9. Possible interactions of the RAFT compound with cancer cell biomacromolecules.

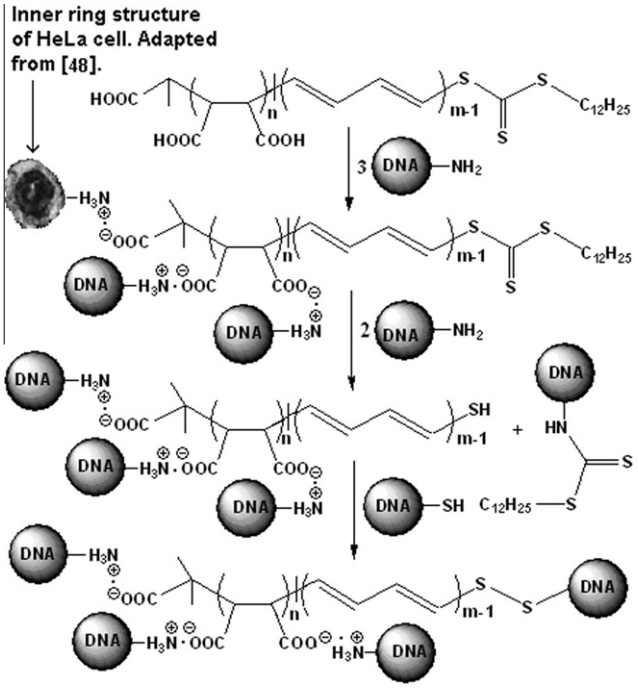

Figure 10. Possible interactions of the PMA–RAFT copolymer with cancer cell biomacromolecules. (See above-mentioned references for further information.)

their roles in various interactions during cancer cell growth and the PMA–RAFT -cell conjugation process will be a subject of our future investigations.

4. Conclusions

This work describes the synthesis of a new carboxyl-trithiocarbonate end-functionalized bioengineering copolymer and the

investigation into the mechanism of its physical and chemical interactions with cancer and normal cells. By using the results of a combination of chemical, biochemical, spectroscopy and statistical analysis methods, we demonstrate that the functional copolymer synthesized by RAFT polymerization of MA exhibits high cytotoxicity and strong apoptotic and necrotic effects toward HeLa cells at relatively low concentrations (around 7.5–75 μg mL^{-1}, IC_{50} = 11.183 μg mL^{-1}) and toward Fibroblast cells at high concentrations (IC_{50} >100 μg mL^{-1}). In the presence of the copolymer, the apoptotic index of cancer cells was significantly higher than that of normal cells. This copolymer also contributed to the lysing of the cell-membrane (necrosis), with relatively high necrotic indexes for the cancer cells. We attributed the observed selective antitumor activity of the PMA–RAFT copolymer to the presence of carboxyl and trithiocarbonate groups, as well as conjugated double bonds, which are responsible for the physical and chemical interactions with biomolecules. The obtained results indicate that the PMA–RAFT copolymer possesses an effective and selective anticancer activity and is a strong candidate for the utilization in clinical cancer therapy.

Acknowledgements

The financial support for this work was provided by TÜBİTAK (Turkish Scientific and Technology Research Council) and the Hacettepe University Scientific Research Foundation through Grants TBAG-2386 and HU-BAB-0201602006, which are gratefully acknowledged.

Supplementary data

Supplementary data associated with this article can be found, in the online version, at http://dx.doi.org/10.1016/j.bmc.2012.05.058.

References and notes

1. Seymour, L. *J. Bioact. Compat. Polym.* **1991**, *6*, 178.
2. Liao, J.; Ottenbrite, R. M. *Controlled Drug Delivery: Challenges and Strategies*; American Chemical Sociaty: Washington, DC, USA, 1997. p 455.
3. Butler, G. B. *Cyclopolymerization and Cyclocopolymerization*; Marcel Dekker: New York, 1992.
4. Akhtar, S. *Gene Ther.* **2006**, *13*, 739.
5. Dittgen, M.; Durrani, M.; Lehmann, K. S. T. P. *Pharma (Paris)* **1997**, *7*, 403.
6. Dimitrov, M.; Lambovi, M.; Shenkov, S.; Dosseva, V.; Baranovski, V. Y. *Acta Pharm.* **2003**, *53*, 25.
7. Saunders, B. R.; Crowther, H. M.; Vincent, B. *Macromolecules* **1997**, *30*, 482.
8. Sawai, T.; Yamazaki, Y.; Ikariyama, Y.; Aizawa, M. *Macromolecules* **1991**, *24*, 2117.
9. Argentiere, S.; Blasi, L.; Ciccarella, G.; Barbarella, G.; Cingolani, R.; Gigli, G. *Macromol. Symp.* **2009**, *281*, 69.
10. El-Subbagh, H. I.; Al-Obaid, A. M. *Eur. J. Med. Chem.* **1996**, *1017*, 31.
11. Andreani, A.; Rambaldi, M.; Andreani, F.; Bossa, R.; Galatulas, I. *Eur. J. Med. Chem.* **1988**, *23*, 385.
12. El-Subbagh, H. I.; Abadi, A. H.; Lehmann, J. *Arch. Pharm. Med. Chem.* **1999**, *332*, 137.
13. Shnur, R. S.; Gallaschun, R. J.; Sungleton, D. H.; Grissom, M.; Sloan, D. E.; Goodwin, P.; McNiff, P. A.; Fliri, F. J. F.; Mangano, M. *J. Med. Chem.* **1975**, *1991*, 34.
14. Kumar, Y.; Green, R.; Borusko, K. Z.; Wise, D. S.; Watring, L. L.; Townsend, L. B. *J. Med. Chem.* **1993**, *36*, 3843.
15. Tricot, G. J.; Jayaram, H. N.; Lapis, E.; Natsumeda, Y.; Nicols, C. R.; Kneebone, P.; Neerema, N.; Weber, G.; Hoffman, R. *Cancer Res.* **1989**, *49*, 3696.
16. Goldstein, B. M.; Leary, J. F.; Farley, B. A.; Marquez, V. E.; Levy, P. C.; Rowley, P. T. *Blood* **1991**, *78*, 593.
17. Husain, A.; Ajmal, M. *Acta Pharm.* **2009**, *59*, 223.
18. Akhtar, T.; Hameed, S.; Al-Masoudi, N. A.; Loddo, R.; La Colla, P. *Acta Pharm.* **2008**, *58*, 135.
19. Abu-Hashem, A. A.; El-Shehry, M. F.; Badria, F. A. *Acta Pharm.* **2010**, *60*, 311.
20. Reddy, L. H. *J. Pharm. Pharmacol.* **2005**, *57*, 1231.
21. Bešić, E. *Acta Pharm.* **2007**, *57*, 249.
22. Lonkar, P.; Dedon, P. C. *Int. J. Cancer* **1999**, *2011*, 128.
23. Tong, R. J.; Cheng, P. C. *Polym. Rev.* **2007**, *47*, 347.
24. *DNA Interactions with Polymers and Surfactants*; Dias, R., Lindman, B., Eds.; John Wiley & Sons: Hoboken, New Jersey, 2008.
25. Greszta, D.; Matyjaszewski, K. *Macromolecules* **1996**, *29*, 7661.
26. *Advances in Controlled/Living Radical Polymerization*; Matyjaszewski, K., Ed.; American Chemical Society: Washington, DC, 2003. Vol. 854.
27. Ross, S. G.; Mueller, A. H. E.; Matyjaszewski, K. In *Controlled/living radical polymerization, ACS Symposium Series 768*; Matyjaszewski, K., Ed.; American Chemical Society: Washington, DC, 2000; p 361.
28. Mayadunne, R. T. A.; Rizzardo, E.; Chiefari, J.; Krstina, J.; Moad, G.; Postma, A.; Thang, S. H. *Macromolecules* **2000**, *33*, 243.
29. Rzayev, J. *Macromolecules* **2009**, *42*, 2135.
30. Huang, K.; Rzayev, J. *J. Am. Chem. Soc.* **2009**, *131*, 6880.
31. Zhao, L.; Byun, M.; Rzayev, J.; Lin, Z. *Macromolecules* **2009**, *42*, 9027.
32. Rzayev, Z. M. O.; Söylemez, E. A. *J. Nanosci. Nanotechnol.* **2011**, *11*, 35231.
33. Rzayev, Z. M. O.; Söylemez, E. A.; Davarcioğlu, B. *Polym. Adv. Technol.* **2011**.
34. Ebeling, B.; Vana, P. *Polymers* **2011**, *3*, 719.
35. Boyer, C.; Stenzel, M. H.; Davis, T. P. *J. Polym. Sci., Part A: Polym. Chem.* **2011**, *49*, 595.
36. Türk, M.; Rzayev, Z. M. O.; Khalilova, S. A. *Bioorg. Med. Chem.* **2010**, *18*, 7975.
37. Türk, M.; Rzayev, Z. M. O.; Kurucu, G. *Health* **2010**, *2*, 51.
38. Rzayev, Z. M. O.; Türk, M.; Uzgören, A. J. *Polym. Sci., Part A: Polym. Chem.* **2010**, *48*, 4285.
39. Kahraman, G.; Türk, M.; Rzayev, Z. M. O.; Unsal, M. E.; Söylemez, E. A. *Collect. Czech. Chem. Commun.* **2011**.
40. Lai, J. T.; Filla, D.; Shea, R. *Macromolecules* **2002**, *35*, 6754.
41. Gaylord, N. G. *J. Macromol. Sci., Part C* **1975**, *13*, 235.
42. Sharabash, M. M.; Guile, R. L. *J. Macromol. Sci., Part A: Pure Appl. Chem.* **1976**, *1017*, 10.
43. Rzayev, Z. M.; Dzhafarov, V. D. *Azerb. Khim. Zh.* **1977**, *5*, 71.
44. Braun, D.; Pomakis, J. *Makromol. Chem.* **1974**, *175*, 1411.
45. Regel, W.; Schneider, C. *Macromol. Chem. Phys.* **1981**, *182*, 237.
46. Ma, W.; Lee, L.; Yang, X.; Wang, X. *J. Appl. Polym. Sci.* **2003**, *88*, 2868.
47. Ryan, M. E.; Hynes, A. M.; Badyal, J. P. S. *Chem. Mater.* **1996**, *8*, 37.
48. Comes, P.; Franke, W. W. *Z. Zellforsch.* **1970**, *107*, 240.